Characterization of NGC 5272, NGC 1904, NGC 3201, and Terzan 3

Paul Hamrick
Avni Bansal
Kalée Tock
Stanford Online High School, 415 Broadway Academy Hall, Floor 2, 8853, Redwood City, CA 94063; paulahamrick@gmail.com; avnibansal2004@gmail.com; kaleeg@stanford.edu

Received July 21, 2021; revised November 9, 2021; accepted November 15, 2021

Abstract Globular clusters are an ideal laboratory for studying and comparing variable stars, since all the variables in a globular cluster formed from the same progenitor gas cloud. Because of this, all of the variables within a given cluster have similar ages, metallicities, reddening, and distances from Earth. Thus we estimated the age, metallicity, reddening, and distance of the clusters NGC 5272, NGC 1904, NGC 3201, and Terzan 3 by doing a visual fit to isochrones. Knowing the characteristics of these clusters as a whole helps us better understand the characteristics of individual variables in these clusters as well. Reddening, metallicity, and age estimates for NGC 1904 and NGC 5272 are consistent with previous literature, but all four of the estimated parameters for Terzan 3 and the metallicity measurement of NGC 3201 differed significantly from literature values. Further research into NGC 3201 and Terzan 3 is recommended.

1.Introduction

Studying the periods of RR Lyraes helps astronomers refine period-metallicity-luminosity relationships (Nemec *et al.* 1994). In addition, knowing the periods of RR Lyraes in a particular globular cluster helps determine how far away the cluster is by the period-luminosity relationship. Specifically, once the period is known, the luminosity can be calculated, and the luminosity can be used to yield the distance by applying the inverse square law and measuring the apparent brightness of the cluster (Catelan *et al.* 2004). In this way, RR Lyraes serve as standard candles.

A challenge in modeling stellar evolution within a cluster is that the temperature and luminosity of stars cannot be measured directly. However, color magnitude diagrams (CMDs) of globular clusters can be used as a proxy for these variables. Within a cluster, the constituent stars can be assumed to have similar age, distance, metallicity, and reddening. This is because all the stars in a given cluster formed together at the same time from the same progenitor gas cloud, so they are roughly the same age and have the same metallicity. Moreover, all stars in a cluster are approximately the same distance from Earth, so their light traverses the same interstellar medium enroute to our telescopes. Therefore, the starlight will be reddened to an extent that depends only on its wavelength.

As a caution, it should be noted that there are some clusters in which there are multiple groups of stars with different ages, such as NGC 6121 (Marino *et al.* 2008). Moreover, clusters with significant reddening tend to show variation in reddening among the stars in them (Bonatto *et al.* 2013). Although there is variation in the reddening and chemical abundances of the stars in some clusters, this is unlikely to affect the model presented here, because the metallicity index that we are using is iron-specific, and the variations in chemical abundances were only found with specific elements which are not iron. In particular, Marino *et al.* found that though other elements or compounds had bimodality in their content, the iron peak-content distribution was found to be homogeneous (Marino *et al.* 2008).

Therefore, assuming that age, metallicity, distance, and reddening are similar for all stars within a cluster, the color magnitude diagram can be used to match the stars to isochrones, which are theoretical models of star populations at a given point in the cluster's evolution. Based on the isochrones, the distance, metallicity, age, and reddening of clusters can be estimated, and these estimates can be refined based on RR Lyrae period-metallicity-luminosity relationships.

Point Spread Function (PSF) photometry was used to identify and measure the stars in NGC 3201, Terzan 3, NGC 5272, and NGC 1904, and create CMDs of these clusters. PSFs are functions that model the brightness profiles of stars in an image. The PSF photometry methods used in this study are Point Spread eXtreme (psx) (Bertin and Arnouts 1996) and DOPhot (Schechter *et al.* 1993). The resulting CMDs were then visually fitted to an appropriate isochrone to estimate the reddening, metallicity, distance, and age of each cluster.

NGC 3201 and Terzan 3 are of particular interest because of their confirmed and hypothesized RR Lyrae populations. NGC 3201 has 160 known RR Lyraes. Astronomers first identified variables in NGC 3201 in 1941 (Wright 1941). Recently, 36 new variables were found (Kaluzny *et al.* 2016). The high incidence of successful variable star searches indicates that NGC 3201 is rich in variables, and further searches may yield yet more variables. Furthermore, even if no new variables are found, it is useful to verify or refine previous period estimates, especially for variables that were discovered around 1941 using older technologies. On the other hand, Terzan 3 does not have any known RR Lyraes, but the preponderance of RR Lyraes in old globular clusters similar to Terzan 3 suggests that a search for RR Lyraes in Terzan 3 may be fruitful.

The four clusters studied here are shown in Figure 1, which was constructed from Las Cumbres Observatory images processed by the Our Solar Siblings pipeline (Fitzgerald *et al.* 2018).

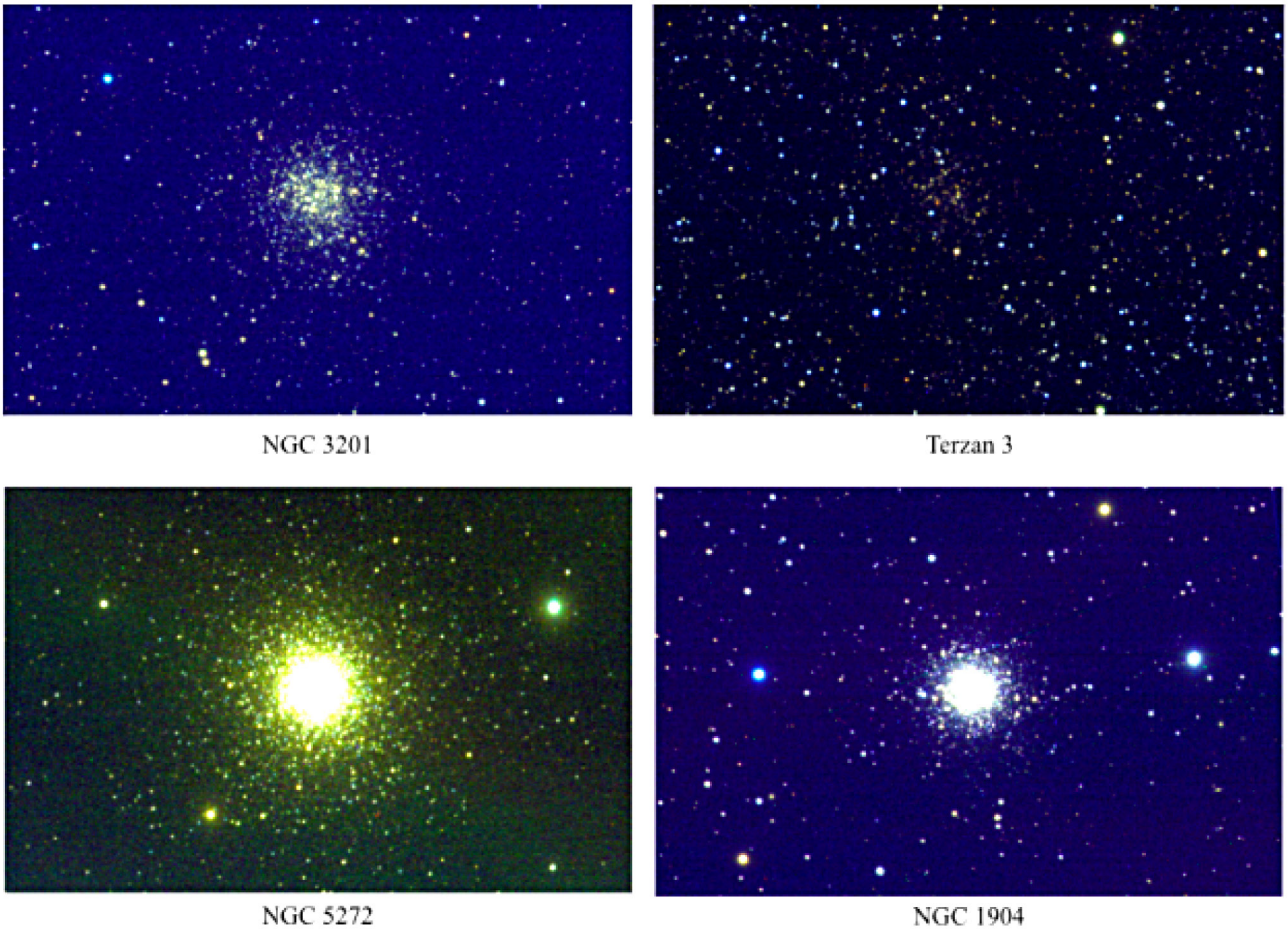

Figure 1. RGB composite images of NGC 3201, Terzan 3, NGC 5272, and NGC 1904.

Table 1. The exposure times of each of the four clusters in each of the eight filters possible with the Las Cumbres Observatory.

Target	*SDSS-up*	*SDSS-gp*	*SDSS-rp*	*SDSS-ip*	*Bessel-B*	*Bessel-V*	*PanSTARRS-w*	*PanSTARRS-z*
Terzan 3	300	200	150	120	300	300	120	60
NGC 3201	300	200	150	120	240	300	120	120
NGC 5272	300	200	200	200	300	230	120	150
NGC 1904	300	300	230	200	300	290	120	200

2. Instruments used

The instruments used were the Las Cumbres Observatory (LCO) telescopes in Cerro Tololo, Chile, in Siding Spring, Australia, in Sutherland, South Africa, and in Fort Davis, Texas. Each telescope is 0.4 meter in diameter and is a Meade 16-inch (40cm) RCS tube and three-element optics, mounted in an LCO equatorial C-ring mounting. The optics are a primary, secondary, and Corrector plate (Meade) with an LCO focus mechanism driving corrector plate/secondary. The instruments on the telescopes are the SBIG STL6303 cameras, which have a 19.5 × 29.5' field of view and a pixel scale of 0.591 arcsec/pixel. The images were taken with each of the eight filters provided by the Las Cumbres Observatory: PanSTARRS-w and PanSTARRS-z (PanSTARRS stands for Panoramic Survey Telescope and Rapid Response System), Bessel B and Bessel V, and SDSS-ip, SDSS-rp, SDSS-gp, and SDSS-up (Sloan Digital Sky Survey). The exposure times in each filter are shown in Table 1.

3. Target selection

We used the VizieR Online Data Catalog and the Clements Catalog (Clement 2017) to find currently observable clusters that were bright enough to be seen by the LCO. We initially chose three clusters with known RR Lyraes (NGC 3201, NGC 1904, NGC 5272) and three clusters with no known RR Lyraes (Terzan 3, 2MASS GC01, IC 1257). However, we decided not to investigate 2MASS GC01 because it was not visible at the time of study. Also, IC 1257 was too dim in the PanSTARRS-w filter using the maximum allowable exposure time of 300 seconds.

4. Procedure for modelling clusters

Images of each of the four target clusters in eight different filters were obtained using LCO telescopes. The images were fed into the Our Solar Siblings pipeline (Fitzgerald *et al.* 2018),

which conducted six different types of photometric reduction on each of the images, including three types of aperture photometry and three types of PSF photometry. Since aperture photometry identifies stars based on brightness, without model-fitting, it is often unable to distinguish closely-packed stars in an image. Thus PSF photometry was chosen for this study because of its higher sensitivity and accuracy: specifically the psx and dop methods mentioned above.

5. Calibration

The photometry data were input to PysoChrone, an Our Solar Siblings software tool written by (Fitzgerald *et al.* 2018), which employs an isochrone model based on (Girardi *et al.* 2020). PysoChrone selected reference stars and calibrated their instrumental magnitudes against magnitudes listed in various databases. The calibration stars are selected as follows. First, stars that were listed in the AAVSO Variable Star Index (Watson *et al.* 2014) were rejected from consideration. Stars are rejected that are too bright, which for the CCD cameras of LCO means that they have above 1,000,000 total aperture counts, with signal-to-noise 1,000. Stars are also rejected that are too dim, meaning that they have below 10,000 total aperture counts, with signal-to-noise less than 100. Depending on filter and availability, different calibration catalogues are used, including the AAVSO Photometric All-Sky Survey (APASS; Henden *et al.* 2016), the Sloan Digital Sky Survey (SDSS; Blanton *et al.* 2017), the he Panoramic Survey Telescope and Rapid Response System (PanSTARRS; (Magnier *et al.* 2016),), and SkyMapper (Wolf *et al.* 2018). Stars that are flagged in these catalogues as being imperfectly measured in any way are rejected. Also, stars need a valid magnitude and error in the filter under consideration and also in the complementary color filter (e.g. V for B to make B–V) in order to be considered as possible reference stars.

PysoChrone used the calibrated star magnitudes and photometry from our images as well as catalog data to generate CMDs of each cluster, using ten different color indexes and magnitude measures. We adjusted the age, metallicity, distance, and reddening to until the corresponding Girardi isochrone had the closest visual match to these CMDs.

6. Results

The images below depict the graphs generated in PysoChrone based on the images in the eight filters provided by Las Cumbres Observatories as described above. PysoChrone was run on each of the clusters investigated, which were Terzan 3, NGC 3201, NGC 1904, and NGC 5272. In Figure 2, blue points represent the stars, while the red lines are the Girardi isochrones. The plots without blue stars are graphs for which the corresponding data were unavailable.

Table 2 shows the parameters of the best-fitting isochrones for each cluster.

7. Analysis of results

The best fitting isochrones we found disagree with the values found by previous papers for Terzan 3. Table 3 shows the values found by previous papers for the clusters we investigated.

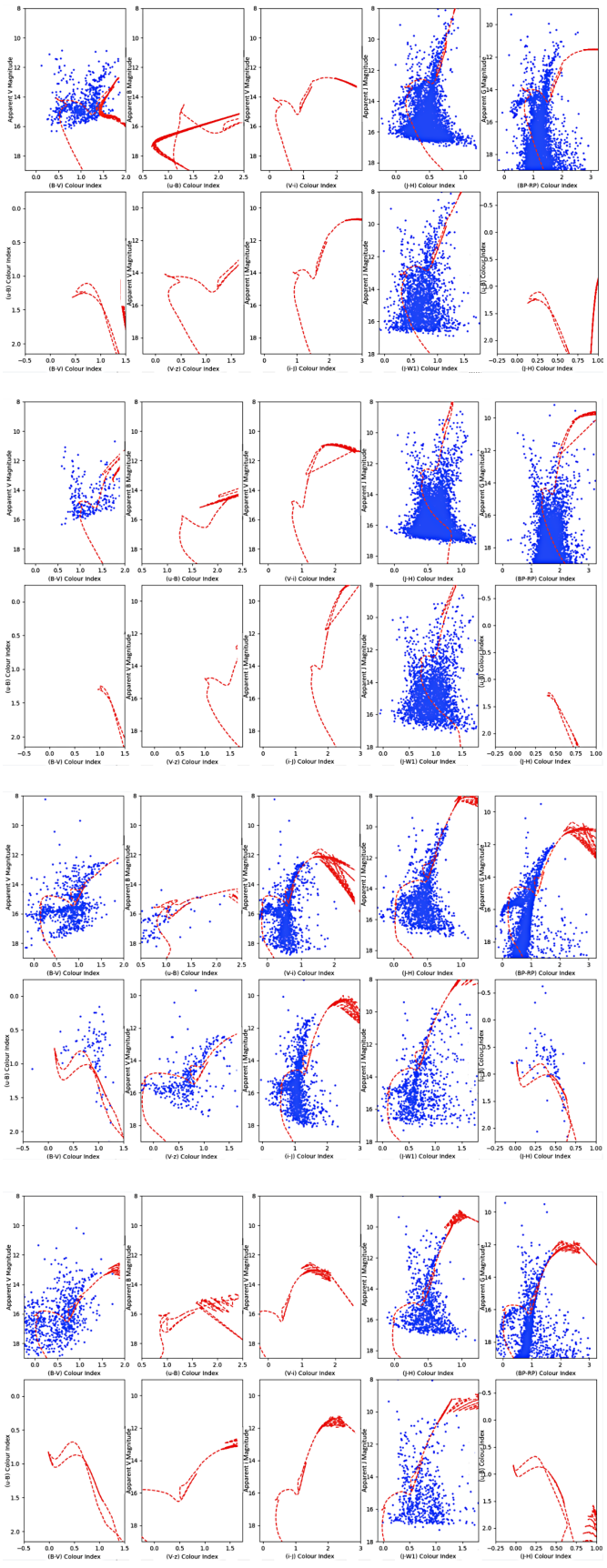

Figure 2. Best fitting isochrones of (from top) NGC 3201, Terzan 3, NGC 5272, and NGC 1904.

Evidently, there is significant disagreement between our values for Terzan 3 (shown in Table 2) and those found using a near infra-red CM diagram by (Valenti *et al.* 2007). While Valenti *et al.* used near infra-red images to derive these results, we have used images in eight different filters ranging from infrared to ultraviolet.

Furthermore, Valenti *et al.* used DAOPhot (Stetson 1987) to analyze images whereas we have used Point Spread eXtractor (Bertin and Arnouts 1996). The difference in photometric reduction technique may account for some of the differences between the values obtained. Photometric reduction of our images with dao found more than twice as many stars as the psx reduction, as measured by the filesize of the resulting photometry text files. However, the dimness of the additional stars identified by dao made their placement on the isochrone uncertain. Therefore, while psx was deemed more reliable in this case, the differing filesizes are indicative of the inherent differences in the two photometric reduction techniques.

In the case of NGC 3201, the magnitude and E(B–V) are reasonably close to the values in the Harris (1996) catalog. However, the metallicity values differ greatly. Furthermore, several other studies using several different methods have all arrived at metallicity values that are closer to the value in the Harris catalog than the value arrived at here, as shown in Table 4. This is likely because the effect of changing metallicity on the isochrone is subtle, and the fit to the isochrone performed here is visual. In other words, insertion of the literature value for the metallicity yields a visual fit that is not significantly different from the one shown in Figure 2.

In the cases of NGC 1904 and NGC 5272, there is strong agreement between our results and those from the Harris catalogue. Minor differences in the metallicity and E(B–V) values can be attributed to the necessarily imprecise nature of visually aligning isochrones to best fit color-magnitude diagrams. Hence, the accumulation of minor inconsistencies in our calibration of metallicity, E(B–V), and age of the cluster may have led to a larger inconsistency in calculating distance in both cases. That this distance measurement is still within 2 kpcs of the Harris catalogue measurement despite error in the case of NGC 1904 should improve confidence in the Harris catalogue values. On the other hand, the distance estimate obtained for NGC 5272 should be taken with a grain of salt.

8. Conclusion

The strong agreement between reddening, metallicity, and age measurements in this study and those previously found for NGC 5272 and NGC 1904 should increase confidence in these parameters. Agreement on the reddening and age values of NGC 3201 should also bolster confidence in those parameters.

Meanwhile, the inexplicable disparity between this study's metallicity values for NGC 3201 and previously found values indicates this cluster's metallicity requires further investigation, ideally using an approach independent from isochrones.

The large disagreement in all four parameters of Terzan 3 calls for further study as well. These disagreements are not surprising since Terzan 3 has been historically understudied. In the absence of a large trove of data it is difficult to pin down the cluster's characteristics. More studies using different techniques to characterize this cluster will eventually result in all the data converging to a narrower, accurate range of characteristics.

Finally, we recommend that the technique of isochrones in estimating distance to clusters should be further analyzed and developed to make this method of finding distances to clusters more reliable and accurate.

Table 2. Characteristics of the four clusters derived by fitting isochrones to CMDs in PysoChrone.

Cluster	*Photometry*	*Distance (kpc)*	*Magnitude (m–M)*	*Age (Billions of Years)*	*Metallicity (Fe/H)*	*Reddening (E(B–V)*
Terzan 3	psx	1.202	10.4	9.5	–0.95	0.60
NGC 3201	psx	4.073	13.05	8.9	–0.4	0.32
NGC 1904	psx	14.8	15.85	8.85	–1.30	0.03
NGC 5272	dop	9.12	14.8	8.7	–1.5	0.23

Table 3. Characteristics of clusters from previous papers.

Cluster	*Distance (kpc)*	*Magnitude (m-M)*	*Metallicity (Fe/H0*	*Reddening E(B-V)*	*Age (Billions of Years)*	*Reference*
Terzan 3	8.1	14.54	–0.82	0.73	—	Valenti *et al.* (2007)
NGC 3201	4.9	14.2	–1.24	0.24	12	Paust *et al*. (2010); Calamida *et al.* (2008)
NGC 1904	12.9	15.59	–1.37	0.01	11.7	Koleva *et al.* (2008)
NGC 5272	33.9	15.07	–1.34	0.01	11.4	Forbes and Bridges (2010)

Table 4. Characteristics of clusters from previous papers.

Metallicity	*Technique*	*Reference*
–1.4	Photoelectric photometry	Zinn (1980)
–1.0	High dispersion spectrometry with echelle spectrograph	Pilachowski *et al.* (1980)
–1.62	121 A mm spectrographs	Zinn and West (1984)

9. Acknowledgements

This research was made possible by AstroImageJ software, which was written by Karen Collins and John Kielkopf, and by PysoChrone, which was written by Michael Fitzgerald.

This work makes use of observations taken by the 0.4-m telescopes of Las Cumbres Observatory Global Telescope Network located in Cerro Tololo, Chile, in Siding Spring, Australia, in Sutherland, South Africa, and in Fort Davis, Texas.

This work utilizes the Harris and Clements catalogs of globular clusters.

This research was made possible through the use of the AAVSO Photometric All-Sky Survey (APASS), funded by the Robert Martin Ayers Sciences Fund, and the International Variable Star Index, maintained by the AAVSO.

References

Bertin, E., and Arnouts, S. 1996, *Astron. Astrophys, Suppl. Ser.*, **117**, 393 (doi: 10.1051/aas:1996164).

Blanton, M. R., *et al.* 2017, *Astron. J.*, **154**, 28 (Sloan Digital Sky Survey IV; https://www.sdss.org/).

Bonatto, C., Campos, F., and Kepler, S. O. 2013, *Mon. Not. Roy. Astron. Soc.*, **435**, 263 (doi: 10.1093/mnras/stt1304).

Calamida, A., *et al.* 2008, in *The Ages of Stars*, Proc. IAU 4, Symp. S258, Cambridge Univ. Press, Cambridge, 189 (doi: 10.1017/S1743921309031846).

Catelan, M., Pritzl, B. J., and Smith, H. A. 2004, *Astrophys. J., Suppl. Ser.*, **154**, 633 (doi: 10.1086/422916).

Clement, C. M. 2017, VizieR On-line Data Catalog: V/150.

Fitzgerald, M. T., McKinnon, D. H., Danaia, L., Cutts, K. R., and Salimpour, M. S. 2018, in *Robotic Telescopes, Student Research and Education Proceedings*, eds. M. Fitzgerald, C. R. Buxner, S. White, RTSRE Proc. 1, RTSRE, San Diego, 217 (https://rtsre.org/index.php/rtsre/issue/view/1).

Forbes, D. A., and Bridges, T. 2010, *Mon. Not. Roy. Astron. Soc.*, **404**, 1203 (doi: 10.1111/j.1365-2966.2010.16373.x).

Girardi, L., Bressan, A., and Bertelli, G., and Chiosi, C. 2000, *Astron. Astrophys, Suppl. Ser.*, **141**, 371 (doi: 10.1051/aas:2000126).

Harris, W. E. 1996, *Astron. J.*, **112**, 1487.

Henden, A. A., Templeton, M., Terrell, D., Smith, T. C., Levine, S., and Welch, D. 2016, VizieR Online Data Catalog: AAVSO Photometric All Sky Survey (APASS) DR9, II/336.

Kaluzny, J., Rozyczka, M., Thompson, I. B., Narloch, W., Mazur, B., Pych, W., and Schwarzenberg-Czerny, A. 2016, *Acta Astron.*, **66**, 31 (https://arxiv.org/abs/1604.01362).

Koleva, M., Prugniel, Ph., Ocvirk, P., Le Borgne, D., and Soubiran, C. 2008, *Mon. Not. Roy. Astron. Soc.*, **385**, 1998 (doi: 10.1111/j.1365-2966.2008.12908.x).

Magnier, E., *et al.* 2016, arXiv preprint, arXiv:1612.05242.

Marino, A. F., Villanova, S., Piotto, G., Milone, A. P., Momany, Y., Bedin, L. R., and Medling, A. M. 2008, *Astron. Astrophys.*, **490**, 625 (doi: 10.1051/0004-6361:200810389).

Nemec, J. M., Nemec, A. F. L., and Lutz, T. E. 1994, *Astron. J.*, **108**, 222 (doi: 10.1086/117062).

Paust, N. E. Q., *et al.* 2010, *Astron. J.*, 139, 476 (doi: 10.1088/0004-6256/139/2/476).

Pilachowski, C. A., Sneden, C., and Canterna, R. 1980, in *Star Clusters*, ed. J. E. Hesser, Proc. IAU Symp. 85, Reidel Publishing Co., Dordrecht, 467.

Schechter, P. L., Mateo, M., and Saha, A. 1993, *Publ. Astron. Soc. Pacific*, **105**, 1342 (doi: 10.1086/133316).

Stetson, P. B. 1987, *Publ. Astron. Soc. Pacific*, **99**, 191 (doi: 10.1086/131977).

Valenti, E., Ferraro, F. R., and Origlia, L. 2007, *Astron. J.*, **133**, 1287 (doi: 10.1086/511271).

Watson, C., Henden, A. A., and Price, C. A. 2014, AAVSO International Variable Star Index VSX (Watson+, 2006–2014; https://www.aavso.org/vsx).

Wright, F. W. 1941, *Bull. Harvard Coll. Obs.*, No. 915, 2.

Wolf, C., *et al.* 2018, *Publ. Astron. Soc. Australia*, **35**, 10 (doi:https://doi.org/10.1017/pasa.2018.5).

Zinn, R. 1980, *Astrophys. J., Suppl. Ser.*, 42, 19 (doi: 10.1086/190643).

Zinn, R., and West, M. J. 1984, *Astrophys. J., Suppl. Ser.*, **55**, 45 (doi: 10.1086/190947).